

We are IntechOpen, the world's leading publisher of Open Access books Built by scientists, for scientists

5,300

Open access books available

131,000

International authors and editors

160M

Downloads

Our authors are among the

154

Countries delivered to

TOP 1%

most cited scientists

12.2%

Contributors from top 500 universities



WEB OF SCIENCE™

Selection of our books indexed in the Book Citation Index
in Web of Science™ Core Collection (BKCI)

Interested in publishing with us?
Contact book.department@intechopen.com

Numbers displayed above are based on latest data collected.
For more information visit www.intechopen.com



Applications of the Effectiveness of Corrosion Inhibitors with Computational Methods and Molecular Dynamics Simulation

Şaban Erdoğan and Burak Tüzün

Abstract

Many experts working in the field of corrosion work in laboratories experimentally with long-term procedures and high costs by making changes in the structures of new corrosion inhibitors or existing inhibitors. Advances in computational chemistry and computer software in recent years combine corrosion prevention studies with theoretical chemistry, enabling fast, cheap and highly accurate research. Researchers working in this field can now predict the electronic, molecular and adsorption properties of anti-corrosion molecules at the molecular level with density functional theory (DFT) and Molecular Dynamics Simulation. This section includes: introduction, corrosion mechanisms, introduction to corrosion inhibitors, density functional theory (DFT) and corrosion applications, Molecular Dynamics Simulation, DFT and Molecular Dynamics Simulation applications of the effectiveness of the selected corrosion inhibitor and results. The theoretical data obtained by both the DFT approach and the molecular dynamics simulation approach showed that the corrosion inhibition efficiency order against iron corrosion for the studied Schiff bases and derivatives can be presented as: DBAMTT > SAMTT > AMTT. HOMO energy value of DBAMTT has $-8,18144$, HOMO energy value of SAMTT has $-8,09001$, and AMTT has $-8,01518$ in HF/6-31++G** basis set.

Keywords: Corrosion, DFT, Molecular Dynamics Simulation, Fe(110), Corrosion inhibitor

1. Introduction

Corrosion prevention studies have been intensified in recent years by the use of many organic compound classes as corrosion inhibitors for metals in acidic environments [1–3]. Both experimental and theoretical studies are carried out on this subject, but due to the fact that experimental studies are expensive and time-consuming, emphasis is placed on theoretical chemistry with software systems that have developed considerably in recent years [4, 5]. Some quantum chemical methods and molecular modeling techniques are carried out to characterize the molecular structure of the inhibitors by determining the effectiveness of corrosion inhibitors and to suggest the mechanisms of their interaction with surfaces [6–8].

Corrosion inhibitors, which are one of the easiest methods of protecting metals against corrosion, are gaining importance day by day [9–11]. The adsorption of

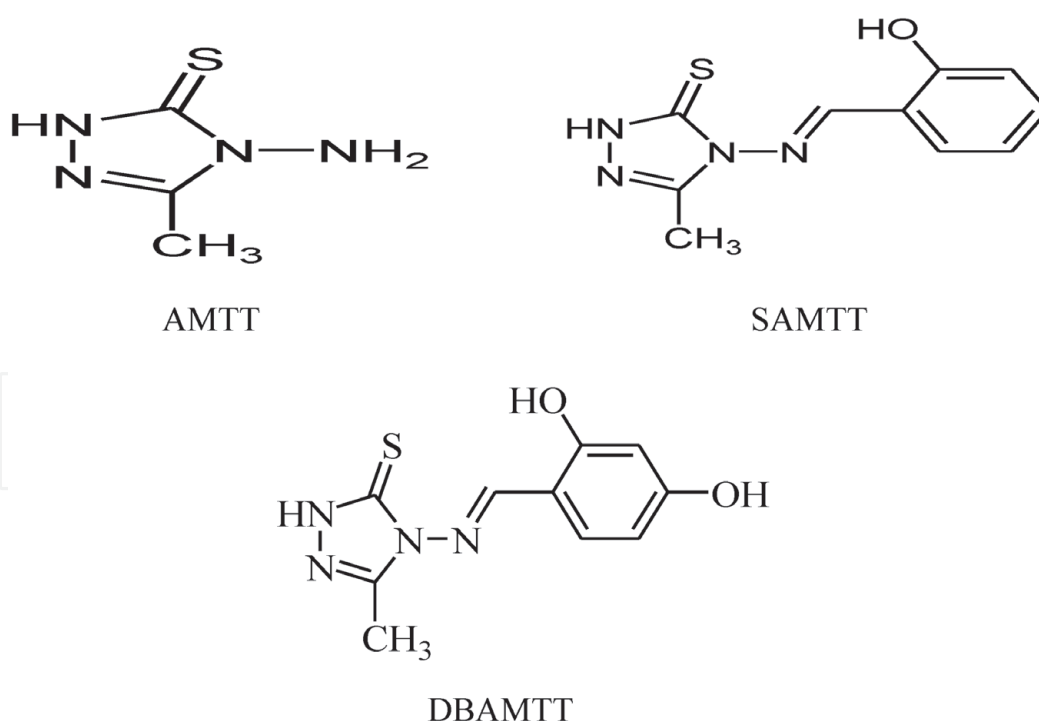


Figure 1.
Chemical molecular structures of studied Schiff bases derivatives.

these molecules depends on many physicochemical properties of the molecules [12–14]. There are many physicochemical properties for the studied molecules to be good inhibitors, such as aromaticity, steric factors, electron density etc. [15–17].

It has been stated in many studies that organic inhibitors contain heteroatoms such as nitrogen, sulfur or oxygen and that congenital double bonded heterocyclic aromatic ring systems are quite good inhibitors for mild steel [18, 19]. Schiff bases are also a very good inhibitor because they have these properties, and many experimental studies are carried out on Schiff bases. In this study, salicylideneamino-3-methyl-1,2,4-triazole-5-thione (SAMTT) and 4-(2,4-dihydroxybenzylideneamino)-3-methyl-1,2,4-triazole-5-thione (DBAMTT) and methyl-1,2,4-triazole-5-thione (AMTT) compounds are theoretically studied [20].

The use of Conceptual density functional theory (DFT) to describe the structure and effectiveness of inhibitors in corrosion processes is becoming a well-known use. With this theory, using the energy of the highest filled molecular orbitals (E_{HOMO}) and the lowest empty molecular orbitals (E_{LUMO}), global chemical descriptors such as hardness [21], electronegativity [22], softness [23], electrophilicity [24] and chemical potential are calculated for corrosion. It provides information about the effectiveness of inhibitors. In this section, determination of the corrosion inhibition efficiency and best inhibitor of the molecules in **Figure 1** on iron corrosion is explained using quantum chemical calculations and molecular dynamics simulations approach.

2. Theory and computational details

Density Functional Theory (DFT), the most common method used to determine the chemical reactivity of molecules, aggregates, and solids, seems to be getting more popular day by day [25]. DFT calculations in this study were made with Gaussian View 5.0.8 program [26] for the preparation of Gaussian 09 [27] input files. The structures of the compounds in the study are calculated with functional B3LYP

[28, 29] based on density functional theory (DFT). High-level 6-311 ++ G (d, p) foundation sets were used in the calculations. This basic set is one of the most accurate basic sets. Calculations in both gas and aqueous phases were also made using SDD, 6-31 ++ G (d, p) and 6-31G base sets, as well as HF and DFT/B3LYP methods, using other levels of theory. One of the reasons to investigate the liquid phase in the study is that the corrosion is higher than the liquid phase. For the liquid phase calculations in the study, Tomasi's polarized continuity model (PCM) and self-consistent reaction area (SCRF) theory were used. These methods model the solvent as a uniform dielectric constant (DC = 78.5) continuity and define the cavity in which the solute is placed as a uniform series of interlocking atomic spheres.

In recent years, DFT methods have been found to be successful in providing insight into chemical reactivity indices such as chemical hardness (η), energy gap ($\Delta E_{\text{gap}} = \text{HOMO-LUMO}$), electronegativity (χ), chemical potential (μ). Fukui functions $f(r)$ [30] in terms of proton affinity (PA), electrophilicity (ω) and nucleophilicity (ϵ) and selectivity [25], spherical descriptors and local descriptors.

Reactivity indices such as electronegativity (χ), chemical hardness (η), and chemical potential (μ) are defined as derivatives of electronic energy (E) with respect to the number of electrons (N) at external potential, $v(r)$. Mathematical operations related to these concepts are given through the following Equations [31].

$$\mu = -\chi = \left(\frac{\partial E}{\partial N} \right)_{v(r)} \quad (1)$$

$$\eta = \frac{1}{2} \left(\frac{\partial^2 E}{\partial N^2} \right)_{v(r)} = \frac{1}{2} = \left(\frac{\partial \mu}{\partial N} \right)_{v(r)} \quad (2)$$

Pearson and Parr were presented the operational and approximate definitions depending on electron affinity (A) and ionization energy (I) of any chemical species (atom, ion or molecule) for chemical hardness, which measures of the resistance of a chemical species to charge transfer, softness (σ) electronegativity and chemical potential in the light of finite differences method [32].

$$\chi = -\mu = \left(\frac{I + A}{2} \right) \quad (3)$$

$$\eta = \frac{I - A}{2} \quad (4)$$

The global softness [33] is defined as the inverse of the global hardness and this quantity is given as in Eq. (4).

$$\sigma = \frac{1}{\eta} \quad (5)$$

Molecular Orbital Theory and Conceptual Density Functional Theory gained a new dimension with the Koopmans theorem [34] presented in the 1930s, and to predict the ionization energy and electron affinities of chemical species, the ionization energy and electron affinity of a molecule approximate the negative values of the orbital energies of HOMO and LUMO, respectively. He predicted that it was equal. Equations (6) and (7) were obtained using Eqs. (3) and (4) to calculate hardness, electronegativity, and chemical potential with the Koopmans theorem.

$$\chi = -\mu = \left(\frac{-E_{\text{HOMO}} - E_{\text{LUMO}}}{2} \right) \quad (6)$$

$$\eta = \left(\frac{E_{LUMO} - E_{HOMO}}{2} \right) \quad (7)$$

The concept of electrophilicity (ω) as a global reactivity index similar to the chemical hardness and chemical potential has been introduced by Parr et al. [35]. This new reactivity descriptor measures the stabilization in energy when the system acquires an additional electronic charge ΔN from the environment. The electrophilicity is defined as in Eq. (8).

$$\omega = \frac{\mu^2}{2\eta} = \frac{\chi^2}{2\eta} \quad (8)$$

The global electrophilicity index (ω) is a descriptor of reactivity that allows a quantitative classification of the global electrophilic nature of a molecule within a relative scale. From the light of this index, electrophilic power of a chemical compounds is associated with its electronegativity and chemical hardness. Nucleophilicity (ε) is physically the inverse of the electrophilicity as is given in the equation below (Eq. (9)).

$$\varepsilon = 1/\omega \quad (9)$$

The solvent effect in the study was examined using the polarized continuity model (PCM) model [36].

3. Results and discussion

The experimental values of the Schiff bases in the study, 4-Amino-3-methyl-1,2,4-triazole-5-thione (AMTT) and its Derivatives (SAMTT and DBAMTT) were obtained by the study [20]. Experimentally, the inhibition activity of these bases was determined as follows: AMTT < SAMTT < DBAMTT.

Quantum chemical descriptors such as E_{HOMO} , E_{LUMO} , Energy gap ($\Delta E = E_{LUMO} - E_{HOMO}$), chemical hardness, softness, electronegativity, chemical potential, proton affinity, electrophilicity and nucleophilicity were calculated and corrosion inhibition was discussed through these parameters. Numerical values of all calculated parameters of Schiff bases and derivatives and their protonated states are given in **Tables 1–4** in gas and water solution.

We will discuss all the parameters in detail below.

3.1 Non-protonated inhibitors

According to the boundary molecular orbit theory FMO, a function of the interaction between HOMO and LUMO levels of the reacting species is defined as chemical reactivity [37]. The molecule's ability to donate electrons to a suitable acceptor with empty molecular orbitals is called E_{HOMO} , and its ability to accept electrons is called E_{LUMO} . The higher the value of the inhibitor's E_{HOMO} , the greater the inhibition efficiency and its presenting electrons to the empty d-orbit of the metal surface. The larger the molecule's ability to accept electrons depends on the lower the value of E_{LUMO} [9]. As a result of the calculations, among the molecules investigated, the lowest energy E_{HOMO} , AMTT had the lowest and DBAMTT the highest corrosion inhibition (**Table 2**). This situation is compatible with causal results. This means that the molecule that tends to adsorb the most on the metal surface is DBAMTT. SAMTT, on the other hand, has a lower number of OH groups

	E_{HOMO}	E_{LUMO}	I	A	ΔE	χ	μ	η	σ	ω	ε
MP2/3-21G* level											
AMTT	-8,04974	4,03357	8,04973	-4,03357	12,08331	2,00808	-2,00808	6,04165	0,16551	0,33371	2,99656
SAMTT	-8,06062	1,85147	8,06062	-1,85147	9,91209	3,10457	-3,10457	4,95604	0,20177	0,97238	1,0284
DBAMTT	-8,00456	2,00631	8,00456	-2,00631	10,01088	2,99912	-2,99912	5,00543	0,19978	0,89849	1,11296
HF/6-31++G**											
AMTT	-8,18144	0,67403	8,18144	-0,67403	8,85547	3,75370	-3,75370	4,42773	0,22585	1,59114	0,62848
SAMTT	-8,09001	0,85635	8,09001	-0,85635	8,94636	3,61683	-3,61683	4,47318	0,22355	1,46221	0,68389
DBAMTT	-8,01518	0,67403	8,01518	-0,67403	8,68921	3,67057	-3,67057	4,34460	0,23017	1,55006	0,64514
HF/6-311++G**											
AMTT	-8,21028	0,64518	8,21028	-0,64518	8,85547	3,78254	-3,78254	4,42773	0,22584	1,61568	0,61893
SAMTT	-8,11695	0,81961	8,11694	-0,81961	8,93656	3,64866	-3,64866	4,46828	0,2238	1,48969	0,67127
DBAMTT	-8,04266	0,65607	8,04266	-0,65607	8,69873	3,69329	-3,69329	4,34936	0,22991	1,56809	0,63771
DFT/6-31++G**											
AMTT	-5,71362	-0,94914	5,71362	0,94914	4,76447	3,33138	-3,33138	2,38224	0,41977	2,32934	0,42931
SAMTT	-5,81294	-2,06944	5,81294	2,06944	3,74349	3,94119	-3,94119	1,87175	0,53426	4,14932	0,24100
DBAMTT	-5,70954	-1,8844	5,70954	1,88440	3,82513	3,79697	-3,79697	1,91256	0,52285	3,76901	0,26532
DFT/6-311++G**											
AMTT	-5,75498	-0,93254	5,75498	0,93254	4,82244	3,34376	-3,34376	2,4112	0,41472	2,31848	0,43131
SAMTT	-5,85566	-2,10019	5,85566	2,10019	3,75547	3,97792	-3,97792	1,87773	0,53255	4,21356	0,23732
DBAMTT	-5,75308	-1,91597	5,75307	1,91596	3,83710	3,83452	-3,83452	1,91855	0,52122	3,83193	0,26096

*, ** is keyword in Gaussian software.

Table 1.
Calculated quantum chemical parameters for non-protonated molecules in gas phase (eV).

	E_{HOMO}	E_{LUMO}	I	A	ΔE	χ	μ	η	σ	ω	ε
MP2/3-21G* level											
AMTT	-8,68975	3,72853	8,68975	-3,72853	12,41829	2,48060	-2,48060	6,20914	0,16105	0,49551	2,01811
SAMTT	-8,59261	1,69011	8,59260	-1,69011	10,28272	3,45124	-3,45124	5,14136	0,19450	1,15836	0,86328
DBAMTT	-8,44594	1,84113	8,44593	-1,84113	10,28707	3,3024	-3,3024	5,14353	0,19441	1,06015	0,94326
HF/6-31++G**											
AMTT	-8,84268	1,24302	8,84268	-1,24302	10,0857	3,79983	-3,79983	5,04285	0,19830	1,43160	0,69852
SAMTT	-8,77166	1,13853	8,77166	-1,13853	9,91019	3,81656	-3,81656	4,95509	0,20181	1,46981	0,68036
DBAMTT	-8,70771	1,14370	8,70771	-1,14370	9,85141	3,78200	-3,78200	4,92570	0,20302	1,45193	0,68874
HF/6-311++G**											
AMTT	-8,85166	1,19867	8,85166	-1,19867	10,05033	3,82649	-3,82649	5,02516	0,19899	1,45687	0,68640
SAMTT	-8,77982	1,08764	8,77982	-1,08764	9,86747	3,84608	-3,84608	4,93373	0,20268	1,49910	0,66706
DBAMTT	-8,71479	1,10070	8,71478	-1,10070	9,81549	3,80703	-3,80703	4,90774	0,20375	1,47659	0,67723
DFT/6-31++G**											
AMTT	-6,15935	-0,51811	6,15934	0,51810	5,64123	3,33873	-3,33873	2,82062	0,35453	1,97600	0,50607
SAMTT	-6,07826	-2,22754	6,07825	2,22754	3,85071	4,15290	-4,15290	1,92536	0,51938	4,47880	0,22327
DBAMTT	-6,02329	-2,04985	6,02328	2,04984	3,97344	4,03657	-4,03657	1,98672	0,50334	4,10070	0,24386
DFT/6-311++G**											
AMTT	-6,19418	-0,55294	6,19417	0,55293	5,64123	3,37355	-3,37355	2,82061	0,35453	2,01744	0,49567
SAMTT	-6,11499	-2,2621	6,11499	2,26210	3,85289	4,18854	-4,18854	1,92644	0,51909	4,55344	0,21961
DBAMTT	-6,06084	-2,08495	6,06083	2,08495	3,97588	4,07289	-4,07289	1,98794	0,50303	4,17227	0,23967

*, ** is keyword in Gaussian software.

Table 2.
Calculated quantum chemical parameters for non-protonated molecules in aqueous solution (eV).

	E_{HOMO}	E_{LUMO}	I	A	ΔE	χ	μ	η	σ	ω	ε
MP2/3-21G* level											
AMTT	-14,5106	1,46017	14,51058	-1,46017	15,97076	6,52520	-6,52520	7,98538	0,12522	2,66601	0,37509
SAMTT	-12,0003	-1,96631	12,00031	1,96631	10,03401	6,98331	-6,98331	5,01700	0,19932	4,86013	0,20575
DBAMTT	-11,7168	-1,89665	11,71677	1,89664	9,82012	6,80671	-6,80671	4,91006	0,20366	4,71799	0,21195
HF/6-31++G**											
AMTT	-14,65644	-2,33911	14,65644	2,33911	12,31733	8,49777	-8,49777	6,15866	0,16237	5,86265	0,17057
SAMTT	-11,90371	-1,92604	11,90371	1,92604	9,97769	6,91487	-6,91487	4,98884	0,20045	4,79224	0,20867
DBAMTT	-11,7132	-1,87270	11,7132	1,87270	9,8405	6,79295	-6,79295	4,92025	0,20324	4,68921	0,21325
HF/6-311++G**											
AMTT	-14,67	-2,33775	14,670046	2,33774	12,3323	8,50389	-8,50389	6,16614	0,16217	5,86397	0,17053
SAMTT	-11,9296	-1,92413	11,929565	1,92413	10,00543	6,92684	-6,92684	5,00271	0,19989	4,79551	0,20852
DBAMTT	-11,7361	-1,87161	11,736091	1,87161	9,86447	6,80385	-6,80385	4,93223	0,20274	4,69283	0,21309
DFT/6-31++G**											
AMTT	-11,7541	-5,59797	11,75405	5,59797	6,15608	8,67601	-8,67601	3,07804	0,32488	12,22745	0,08178
SAMTT	-9,71128	-5,72859	9,71127	5,72858	3,98269	7,71993	-7,71993	1,99134	0,50217	14,96409	0,06682
DBAMTT	-9,49168	-5,48341	9,49167	5,48340	4,00826	7,48754	-7,48754	2,00413	0,49896	13,98691	0,07149
DFT/6-311++G**											
AMTT	-11,7902	-5,63498	11,790242	5,63497813	6,155264	8,71261	-8,71261	3,077632	0,324925	12,33246	0,081087
SAMTT	-9,76216	-5,76206	9,7621615	5,7620563	4,000105	7,762109	-7,762109	2,000053	0,499987	15,06219	0,066391
DBAMTT	-9,53957	-5,51824	9,5395706	5,51824036	4,02133	7,528905	-7,528905	2,010665	0,497348	14,09594	0,070942

*, ** is keyword in Gaussian software.

Table 3.
Calculated quantum chemical parameters for protonated molecules in gas phase (eV).

	E_{HOMO}	E_{LUMO}	I	A	ΔE	χ	μ	η	σ	ω	ε
MP2/3-21G* level											
AMTT	-10,6512	2,63136	10,65116	-2,63136	13,28253	4,00990	-4,00990	6,64126	0,15057	1,21056	0,82606
SAMTT	-9,2582	1,21309	9,25820	-1,21309	10,4713	4,02255	-4,02255	5,23564	0,19099	1,54526	0,64713
DBAMTT	-9,0835	1,35350	9,08350	-1,35350	10,43701	3,865	-3,865	5,21850	0,19162	1,43127	0,69867
HF/6-31++G**											
AMTT	-10,69307	1,15159	10,69307	-1,15159	11,84466	4,77074	-4,77074	5,92233	0,16885	1,92153	0,52041
SAMTT	-9,16160	1,08275	9,16160	-1,08275	10,24435	4,03942	-4,03942	5,12217	0,19523	1,59277	0,62783
DBAMTT	-9,01874	1,08656	9,01874	-1,08656	10,1053	3,96609	-3,96609	5,05265	0,19791	1,55659	0,64242
HF/6-311++G**											
AMTT	-10,698	1,11458	10,69796	-1,11458	11,81256	4,79169	-4,79169	5,90627	0,16931	1,94372	0,51447
SAMTT	-9,18664	1,03948	9,18663	-1,03948	10,22612	4,07357	-4,07357	5,11306	0,19557	1,62271	0,61625
DBAMTT	-9,03616	1,05036	9,03615	-1,05036	10,08652	3,99289	-3,99289	5,04326	0,19828	1,58064	0,63265
DFT/6-31++G**											
AMTT	-7,79014	-1,51623	7,79013	1,51623	6,27390	4,65318	-4,65318	3,13695	0,31878	3,45113	0,28975
SAMTT	-6,90168	-2,68415	6,90167	2,68415	4,21752	4,79291	-4,79291	2,10876	0,47421	5,44680	0,18359
DBAMTT	-6,74031	-2,48605	6,74031	2,48605	4,25426	4,61318	-4,61318	2,12713	0,47011	5,00238	0,19990
DFT/6-311++G**											
AMTT	-7,81953	-1,54916	7,81952	1,54915	6,27036	4,68434	-4,68434	3,13518	0,31896	3,49948	0,28575
SAMTT	-6,95991	-2,71926	6,95991	2,71925	4,24065	4,83958	-4,83958	2,12032	0,47162	5,5231	0,18105
DBAMTT	-6,79528	-2,52224	6,79528	2,52224	4,27303	4,65876	-4,65876	2,13651	0,46805	5,07930	0,19687

*, ** is keyword in Gaussian software.

Table 4.
Calculated quantum chemical parameters for protonated molecules in aqueous solution (eV).

than DBAMTT, so its corrosion inhibition efficiency is less than DBAMTT. **Figure 2** shows the areas where the activities of molecules are high. It is seen that these areas are the regions where nitrogen is present.

The ΔE approach, defined as the HOMO - LUMO energy deficit, is a very important stability index and provides the necessary theoretical models to make explanations about the structure and conformation in molecular systems. In order to have a high inhibition efficiency, the ΔE value should be low [47–49]. When the investigated molecules were compared, it was seen that there was a DBAMTT molecule in the smallest HOMO-LUMO gap (8,68921 eV obtained by HF method) as seen in **Table 2**. This means that the DBAMTT molecule has a tendency to adsorb more on the metal surface than other molecules and can be expected to be a very good corrosion inhibitor.

Electronegativity indicates the strength of atoms in a molecule to attract bonding electrons [50]. The higher the electronegativity value of the molecule, the more the atoms in the molecule will attract the bond electrons. This will cause the inhibitor activity of the molecule to decrease [51].

The reason for not making a detailed analysis on the dipole moment μ , it should be stated first that there is no consensus on the relationship between dipole moment and inhibition efficiency in literature [7, 11, 38–41]. The results obtained in the

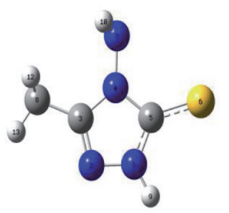
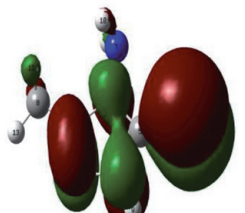
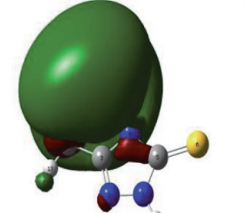
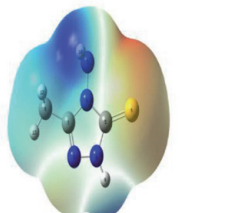
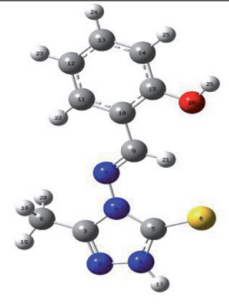
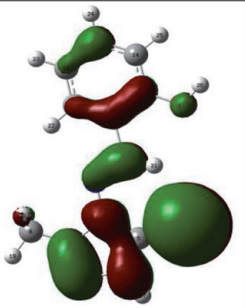
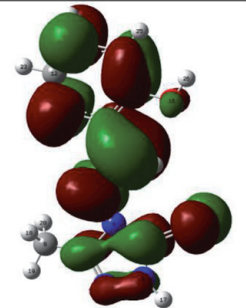
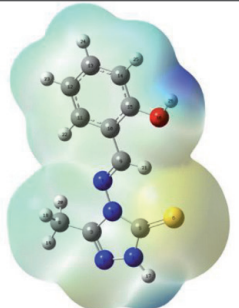
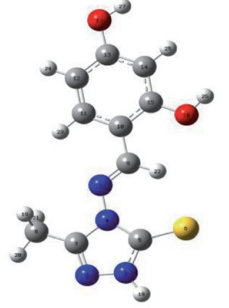
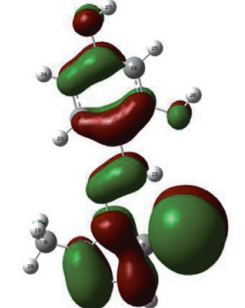
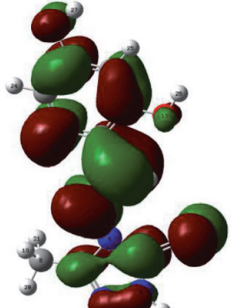
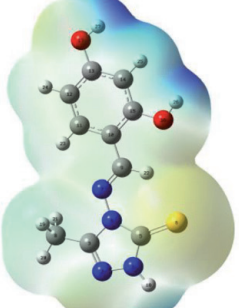
Inhibitor	Optimized Structure	HOMO	LUMO	ESP
AMTT				
SAMTT				
DBAMTT				

Figure 2. The optimized structures, HOMO_s, LUMO_s and electrostatic potential structures of nonprotonated inhibitor molecules using DFT/6–311++G^{**} calculation level.

study also show that there is no significant result between μ and inhibition efficiency and that it confirms the previous studies.

One of the ways to measure molecular stability and reactivity is Absolute hardness, η , and softness σ , where a hard molecule has a fairly large energy gap and a soft molecule has a small energy gap. Soft molecules are more reactive than hard molecules because they easily donate electrons to the receiver. While performing a simple electron transfer from the adsorption molecule, the transfer takes place from the part where the σ value of the molecule is highest [42]. In corrosion systems, the metal behaves like a Lewis acid and while it is soft acid, the inhibitor acts as a Lewis base and the more soft base inhibitors are, the more these metals have an effect on acidic corrosion. In this case, when **Table 2** dec-I data were examined, it was seen that the DBAMTT inhibitor had the highest σ value and this was an expected result when compared with the experimental results.

When iron and inhibitor approach each other, electrons flow from low χ (inhibitor) to high χ (iron) until their chemical potential or electronegativity is equal. As a first approximation, the fraction of electrons transferred, N , is given by Eq. (10).

$$\Delta N_{\max} = \frac{\chi_{Fe} - \chi_{inh}}{2(\eta_{Fe} + \eta_{inh})} \quad (10)$$

In the Hard Soft Acid Base (HSAB) theory [43], it was determined that iron behaves like Lewis acid, so the difference in electronegativity drives the electron transfer and the sum of the hardness parameters acts as a resistance. This is calculated using the fraction of transferred electrons assuming $I = A$ for a metallic mass, using a theoretical value $\chi_{Fe} = 7 \text{ eV}$ [44] for cast iron's electronegativity and a global hardness $Fe = 0$. [45] In this study, the number of electrons transferred (ΔN_{\max}) of the compounds under the probe is calculated and the results are shown in **Tables 5** and **6**. According to Lukovits et al. [46], if $\Delta N < 3.6$, inhibition efficiency increased with increasing ability to donate electrons at the metal surface. A value of $\Delta N_{\max} < 3.6 \text{ eV}$ indicates the tendency of a molecule to donate electrons to the metal surface. The results in **Tables 5** and **6** revealed that the molecules under the probe act as electron donors outside the protonated AMTT, SAMTT, and DBAMTT species in the gas phase and at the B3LYP/6-31 ++ G (d, p) theory level. Acting as an electron acceptor. The results show that the highest fraction of transferred electrons, ΔN_{\max} , is associated with the best inhibitor (DBAMTT), while the least fraction is associated with the inhibitor with the least inhibitory activity (AMTT). In any case, the ability of inhibitor molecules to donate electrons follows the order DBAMTT > SAMTT > AMTT. These results are in good agreement with experimental studies.

Recently, according to the theory presented by Gomez et al. [47], provided that both electron transfer to the molecule and recycling from the molecule are simultaneously, the energy change and the hardness of the molecule change in direct proportion (Eq. (11)).

$$\Delta E_{back-donation} = -\frac{\eta}{4} \quad (11)$$

Eq. (11) implies that when $\eta > 0$ or $\Delta E_{b-d} < 0$, back-donation from molecule to metal is energetically preferred. The results reported in **Table 5** show that $\Delta E_{b-d} < 0$, therefore charge transfer to a molecule followed by re-release from the molecule is energetically favorable. Assuming that the inhibition efficiency should increase when the molecule has better adsorption on the metal surface, the inhibition efficiency should increase when the stabilization energy resulting from the interaction between the metal surface and the inhibitor increases. As expected and

	Gas phase (non-protonated)				Aqueous (non-protonated)			
	ΔN_{\max}	$\Delta\psi$	ΔE_{b-d}	E	ΔN_{\max}	$\Delta\psi$	ΔE_{b-d}	E
MP2/3-21G*								
AMTT	0,41312	-1,03114	-1,51041	-729.44927	0,36393	-0,82237	-1,55229	-729.47345
SAMTT	0,39299	-0,76545	-1,23901	-1070.53989	0,34511	-0,61237	-1,28534	-1070.55704
DBAMTT	0,39965	-0,79948	-1,25136	-1145.09747	0,35944	-0,66454	-1,28588	-1145.11973
HF/6-31++G**								
AMTT	0,36658	-0,59502	-1,10693	-732.38094	0,31729	-0,5077	-1,26071	-732.40847
SAMTT	0,37816	-0,63969	-1,11829	-1074.66910	0,32122	-0,51131	-1,23877	-1074.69232
DBAMTT	0,38316	-0,63787	-1,08615	-1149.53371	0,32665	-0,52558	-1,23143	-1149.56242
HF/6-311++G**								
AMTT	0,36332	-0,5845	-1,10693	-732.47119	0,315761	-0,50103	-1,25629	-732.49798
SAMTT	0,37501	-0,6284	-1,11707	-1074.81934	0,319627	-0,50404	-1,23343	-1074.84198
DBAMTT	0,38013	-0,6285	-1,08734	-1149.70469	0,325298	-0,51933	-1,22694	-1149.73270
DFT/6-31++G**								
AMTT	0,76999	-1,41241	-0,59556	-735.11261	0,64902	-1,18812	-0,70515	-735.135390
SAMTT	0,81709	-1,24967	-0,46794	-1079.51087	0,73937	-1,05253	-0,48134	-1079.52795
DBAMTT	0,83736	-1,34105	-0,47814	-1154.73730	0,74581	-1,10508	-0,49668	-1154.75993
DFT/6-311++G**								
AMTT	0,75817	-1,38603	-0,6028	-735.21174	0,64284	-1,16562	-0,70515	-735.23387
SAMTT	0,80471	-1,21595	-0,46943	-1079.67813	0,7297	-1,02576	-0,48161	-1079.69497
DBAMTT	0,82496	-1,3057	-0,47964	-1154.92623	0,73621	-1,07749	-0,49699	-1154.94853

*, ** is keyword in Gaussian software.

Table 5. Calculated quantum chemical parameters (ΔN_{\max} , $\Delta\psi$, and ΔE_{b-d} (in eV) and the optimized energies (E in hartree) of the non-protonated molecules under probe in gas phase and in aqueous solution (eV).

	Gas phase (protonated)				Aqueous (protonated)			
	ΔN_{\max}	$\Delta\psi$	ΔE_{b-d}	E	ΔN_{\max}	$\Delta\psi$	ΔE_{b-d}	E
MP2/3-21G*								
AMTT	0,02972	-0,00706	-1,99635	-729.81437	0,22511	-0,33656	-1,66032	-729.89906
SAMTT	0,00166	-1,4E-05	-1,25425	-1070.89826	0,28434	-0,42331	-1,30891	-1070.97158
DBAMTT	0,01968	-0,0019	-1,22752	-1145.45825	0,30037	-0,47084	-1,30463	-1145.53527
HF/6-31++G**								
AMTT	-0,1216	-0,09106	-1,53967	-732.744808	0,18820	-0,20978	-1,48058	-732.83143
SAMTT	0,00853	-0,00036	-1,24721	-1075.03491	0,28899	-0,4278	-1,28054	-1075.11235
DBAMTT	0,02103	-0,00218	-1,23007	-1149.90218	0,30023	-0,45543	-1,26316	-1149.98316
HF/6-311++G**								
AMTT	-0,12195	-0,0917	-1,54154	-732.83585	0,18694	-0,20642	-1,47657	-732.922210
SAMTT	0,00731	-0,00027	-1,25068	-1075.18616	0,28617	-0,41873	-1,27826	-1075.26330
DBAMTT	0,01988	-0,00195	-1,23306	-1150.07416	0,29813	-0,44826	-1,26082	-1150.15477
DFT/6-31++G**								
AMTT	-0,27225	-0,22815	-0,76951	-735.47180	0,37406	-0,43892	-0,78424	-735.557070
SAMTT	-0,18077	-0,06507	-0,49784	-1079.87080	0,523313	-0,57750	-0,52719	-1079.94506
DBAMTT	-0,12163	-0,02965	-0,50103	-1155.10077	0,56104	-0,66955	0,53178	-1155,17815
DFT/6-311++G**								
AMTT	-0,27824	-0,23825	-0,76941	-735.57066	0,369302	-0,42759	-0,7838	-735.65562
SAMTT	-0,19052	-0,0726	-0,50001	-1080.03816	0,509454	-0,55032	-0,53008	-1080.11220
DBAMTT	-0,13153	-0,03478	-0,50267	-1155.28982	0,54791	-0,64139	-0,53413	-1155.36693

*, ** is keyword in Gaussian software.

Table 6. Calculated quantum chemical parameters (ΔN_{\max} , $\Delta\psi$, and ΔE_{b-d} (in eV) and the optimized energies (E in hartree) of the protonated molecules under probe in gas phase and in aqueous solution (eV).

in line with the experimental results [48], the calculated values of ΔE_{b-d} tend to: DBAMTT > SAMTT > AMTT.

In the theoretical studies, the ESP calculations of the molecules show the regions where the electron density is high in the molecule [49]. For this reason, molecules interact chemically by donating electrons on atoms with higher electron density. It is seen that the electron density of the sulfur atom is higher than the other atoms in the calculated molecules. For this reason, they try to be good inhibitors by interacting chemically over the molecular sulfur atom [50].

Apart from these, another important property, Sastri and Perumareddi [49] discovered by using the following equation molecule-metal interaction energy ($\Delta\psi$) can be calculated (14).

$$\Delta\psi = -\frac{(\chi_{Fe} - \chi_{inh})^2}{4(\eta_{Fe} + \eta_{inh})} \quad (12)$$

When the results are examined, molecule-metal interaction $|\Delta\psi|$, is respectively as DBAMTT > SAMTT > AMTT (Tables 5 and 6). In addition, the initial molecule-metal interaction energy ($\Delta\psi$) order is again DBAMTT > SAMTT > AMTT.

3.2 Protonated inhibitors

The enthalpy of the reaction of a chemical species in the gas phase with the H⁺ ion is defined as the affinity of protons (PA) [50, 52]. PA gives information about the ability of chemical compounds to donate or accept electrons and the degree of alkalinity. Compounds containing heteroatoms such as oxygen and nitrogen tend to protonate very well in acidic environments and aqueous solutions. Tables 7 and 8 shows the PA values of the compounds in this study with different calculation methods in gas and aqueous solution. When PA values and excision activities were compared, it was determined that the efficiency ranking was DBAMTT > SAMTT > AMTT and was consistent with the experimental result.

	MP2/3 – 21G*	HF/6–31++G**	HF/6–311++G**	DFT/6–31++G**	DFT/6–311++G**
AMTT	-2,57861	-2,54504	-2,56663	-2,41766	-2,41038
SAMTT	-2,3954	-2,59792	-2,62543	-2,43794	-2,44059
DBAMTT	-2,46101	-2,67045	-2,69756	-2,53419	-2,5375

*, ** is keyword in Gaussian software.

Table 7.
 Calculated proton affinity values of studied quinoline derivatives in gas phase using different calculation levels.

	MP2/3-21G*	HF/6–31++G**	HF/6–311++G**	DFT/6–31++G**	DFT/6–311++G**
AMTT	-4,22579	-4,15365	-4,18822	-4,11906	-4,12071
SAMTT	-3,92444	-4,07382	-4,10900	-3,99439	-3,99767
DBAMTT	-3,95166	-4,09308	-4,12942	-4,02454	-4,02952

*, ** is keyword in Gaussian software.

Table 8.
 Calculated proton affinity values of studied quinoline derivatives in aqueous solution using different calculation levels.

The following equation is used to calculate the PA values of Schiff bases compounds.

$$PA = E_{(\text{pro})} - (E_{(\text{non-pro})} + E_{H^+}) \quad (13)$$

In the above equation, $E_{\text{non-pro}}$ and E_{pro} are energies of non-protonated and protonated inhibitors, respectively. E_{H^+} is the energy of the H^+ ion and is calculated in the figure below.

In the high calculation methods selected in the study, the protonated inhibitors have lower E_{HOMO} values compared to their non-protonated states, and the order is respectively DBAMTT, SAMTT, AMTT, and these results given in **Table 3** are consistent with the experimental inhibition efficiency.

Agreement of E_{HOMO} values with experimental data E_{LUMO} and T.E. and there is a correlation between these parameters and the inhibition efficiency. When the ΔE values were examined, it was seen that the lowest value belonged to DBAMTT and it was determined that it was the most intrusive (9,8405 eV).

In addition, when **Tables 2** and **3** are examined, it is seen that protonated compounds have higher μ than non-protonated compounds. Similarly, this verification was made for chemical hardness. The results show that the calculations show that non-protonated inhibitors have a more positive ΔN value than the protonated inhibitor. The DBAMTT molecule, on the other hand, has the highest ΔN value in each round, confirming that it has the same highest inhibitory properties as experimental data.

3.3 Solvent effect

The greater occurrence of the corrosion phenomenon in the solvent phase indicates that the solvent phase in the process may be important. Inhibitors may show different properties in a vacuum or in another solvent [1, 27, 50–51]. In the study, the solvent effect on the molecular structure of the solute was calculated by the polarized continuity model (PCM) model [45]. In the PCM model, the solvent is treated as a continuous dielectric medium, and the solute is considered a molecule trapped in a cavity surrounded by the solvent. In the Gaussian 09 program, CPCM, a special version of PCM based on integral equation formalism, was used together with HF/6-31 ++ G (d, p) to examine the solvent effect. When the results are examined, a small increase is shown for the values of E_{HOMO} , E_{LUMO} , ΔE , T.E., P_i , MV , i and g , while a rather small decrease is shown for values of v and ΔN . For the molecule in this study, it was determined that the quantum chemical parameters calculated in the presence of a solvent (water) and in the gas phase did not differ significantly (**Table 5**).

3.4 Molecular dynamic simulations

Monte Carlo simulations can be used to predict interactions between inhibitor molecules and metal surface. In the study, the most stable low energy adsorption configurations of AMTT, SAMTT, DBAMTT on the Fe (110) surface were induced by Monte Carlo simulation and the configurations are shown in **Figure 3**. Outputs and descriptors, including total adsorption, solid adsorption and deformation energies are given in **Table 9**. Adsorption energy is attributed to the energy released during relaxed adsorbate components adsorbed on the substrate. Adsorption energy is the addition of solid adsorption and deformation energies of the adsorbate component. Higher values of negative adsorption energy indicate the presence of a more stable and stronger interaction between a metal and an inhibitor molecule. Monte Carlo simulation and DFT calculation results showed

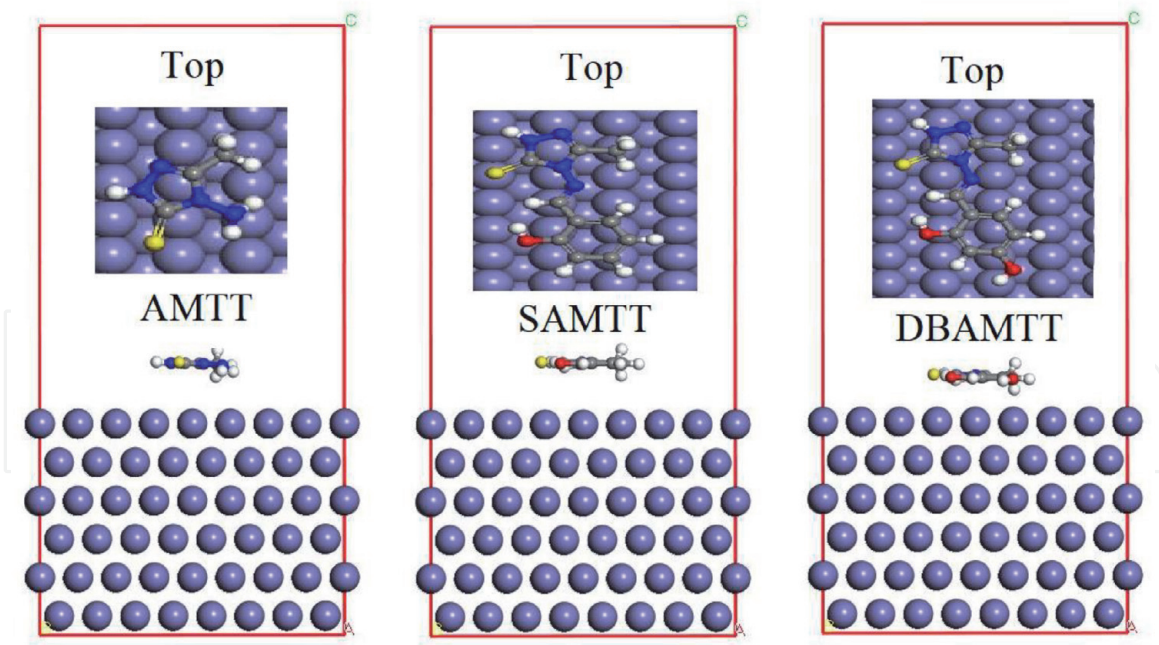


Figure 3. Top and side views of the most stable low energy configurations for the adsorption of three inhibitors on Fe (110) interface obtained using Monte Carlo simulations.

Inhibitor	Total energy	Adsorption energy	Rigid adsorption energy	Deformation energy	dE_{ad}/dN_i	IE (%)
AMTT	-33,84	-164,48	-71,85	-92,63	-164,48	73
SAMTT	-172,27	-352,70	-138,95	-213,74	-352,70	93
DBAMTT	-196,85	-383,50	-143,74	-239,76	-383,50	94

Table 9. Experimental inhibition efficiencies, IE (%) and the outputs and descriptors calculated by the Monte Carlo simulation for adsorption AMTT, SAMTT, DBAMTT of on Fe (110) (in kcal Mol⁻¹).

us once again that the corrosion inhibition efficiency was in the form of DBAMTT, SAMTT and AMTT, respectively, and it was seen to confirm the experimental results [28].

4. Conclusions

DBAMTT, SAMTT, and AMTT molecules used in this theoretical study were synthesized by M. Saravana Kumar et al. In order to predict the corrosion inhibition activities of Schiff bases and derivatives against the corrosion of iron metal, density functional theory with different basic sets and molecular dynamics simulation approach were used in Hartree Fock (HF), B3LYP. Quantum chemical calculations of the non-protonated and protonated structures of the molecules examined in this study were made in both gas phase and aqueous solution. At the end of the study, the following results are given in summary.

- The studied Schiff bases and derivatives are thought to be very important in preventing the corrosion of iron metal.
- The theoretical data obtained by both the DFT approach and the molecular dynamics simulation approach showed that the corrosion inhibition efficiency

order against iron corrosion for the studied Schiff bases and derivatives can be presented as: DBAMTT > SAMTT > AMTT.

- According to the binding energies presented in **Table 8**, it was determined that among the molecules examined, DBAMTT was the most effective inhibitor of iron corrosion and the calculated binding energies were similar to the experimental data.
- Results and interpretations resulting from the study can give an idea for new corrosion inhibitor studies in the following processes and help in the selection of corrosion inhibitors.

Acknowledgements

This research was made possible by TUBITAK ULAKBIM, High Performance and Grid Computing Center (TR-Grid e-Infrastructure).

Authors Contribution

Şaban Erdoğan performed the calculations. Şaban Erdoğan and Burak Tüzün discussed and analyzed the results. All authors equally contributed to preparation of the manuscript. All the authors have read and approved the final manuscript.

Funding information

This research received no specific grant from any funding agency in the public, commercial, or not-for-profit sectors.

Compliance with ethical standards

Conflict of interest the authors declare that they have no conflict of interest.

Availability of data and materials

The datasets generated during the current study are available from the corresponding author on reasonable request.

IntechOpen

Author details

Şaban Erdoğan^{1*} and Burak Tüzün²

1 Department of Nutrition and Dietetics, Faculty of Health Sciences, Yalova University, Yalova, Turkey

2 Department of Chemistry, Faculty of Science, Cumhuriyet University, Sivas, Turkey

*Address all correspondence to: saban.erdogan@yalova.edu.tr

IntechOpen

© 2021 The Author(s). Licensee IntechOpen. This chapter is distributed under the terms of the Creative Commons Attribution License (<http://creativecommons.org/licenses/by/3.0>), which permits unrestricted use, distribution, and reproduction in any medium, provided the original work is properly cited. 

References

- [1] N. Hackerman, *Langmuir*. 3 (1987) 922-924.
- [2] P. Marcus, *Corrosion mechanisms in theory and practice*. 2002, New York Inc.: Marcel Dekker.
- [3] M.S. Masoud, M.K. Awad, M.A. Shaker, M.M.T. El-Tahawy, *Corr. Sci.* 52 (2010) 2387-2396.
- [4] C. Loganayagi, C. Kamal, M.G. Sethuraman, *ACS Sustainable Chem. And Eng.* 2 (2014) 606-613.
- [5] I.B. Obot, S. Kaya, C. Kaya, B. Tüzün, *Res. Chem. Int.* 42 (2016) 4963-4983.
- [6] S. Kaya, P. Banerjee, S.K. Saha, B. Tüzün, C. Kaya, *RSC Advances*. 6 (2016) 74550-74559.
- [7] N.O. Obi-Egbedi, I.B. Obot, Mohammad I. El-Khaiary, *J. Mol. Struct.* 1002 (2011) 86-96.
- [8] Z.S. Safi, S. Omar, *Chem. Phys. Lett.* 610 (2014) 321-330.
- [9] S Kaya, L Guo, C Kaya, B Tüzün, IB Obot, R Tourir, N Islam, *Journal of the Taiwan Institute of Chemical Engineers* 65 (2016) 522-529
- [10] Hany M. Abd El-Lateef, Ahmed M. Abu-Dief, Mounir A.A. Mohamed, *J. Mol. Struct.* 1130 (2017) 522-542.
- [11] S. Kaya, B. Tüzün, C. Kaya, I.B. Obot, *J. Taiwan Inst. Chem. Eng.* 58 (2016) 528-535.
- [12] N.A. Wazzan, I.B. Obot, S. Kaya, *J. Mol. Liq.* 221 (2016) 579-602.
- [13] S.A. Umoren, I.B. Obot, A. Madhankumar, Z.M. Gasem, *Carbohydrate Polymers*. 124 (2005) 280-291.
- [14] Fei Yu, Shougang Chen, Yan Chen, Houmin Li, Lejiao Yang, Yuanyuan Chen, Yansheng Yin, *J. Mol. Struct.* 982 (2010) 152-161.
- [15] Hadi Behzadi, Ali Forghani, *J. Mol. Struct.* 1131 (2017) 163-170.
- [16] Hany M. Abd El-Lateef, Ahmed M. Abu-Dief, Mounir A.A. Mohamed, *J. Mol. Struct.* 1130 (2017) 522-542.
- [17] M. Lebrini, M. Lagnere, H. Vezin, M. Traisnel, F. Bentiss, *Corr. Sci.* 49 (2007) 2254-2269.
- [18] S.K. Saha, A. Dutta, P. Ghosh, D. Sukul, P. Banerjee, *Phys. Chem. Chem. Phys.* 17 (2015) 5679-5690.
- [19] A. Dutta, S.K. Saha, P. Banerjee, D. Sukul, *Corr. Sci.* 98 (2015) 541-550.
- [20] Kumar, M. S., Kumar, S. L. A., & Sreekanth, A. (2012). Anticorrosion potential of 4-amino-3-methyl-1, 2, 4-triazole-5-thione derivatives (SAMTT and DBAMTT) on mild steel in hydrochloric acid solution. *Industrial & engineering chemistry research*, 51(15), 5408-5418
- [21] S. Kaya, C. Kaya, *Mol. Phys.* 113 (2015) 1311-1319.
- [22] S. Kaya, C. Kaya, *Computational and Theoretical Chemistry*. 1052 (2015) 42-46.
- [23] S. Kaya, C. Kaya, *Computational and Theoretical Chemistry*. 1060 (2015) 66-70.
- [24] P.K. Chattaraj, U. Sarkar, D.R. Roy, *Chem. Rev.* 106 (2006) 2065-2091.
- [25] H. Chermette, *J. Comp. Chem.* 20 (1999) 129-154.
- [26] R. D. Dennington, T. A. Keith, C. M. Millam, *GaussView 5.0*, Wallingford CT, 2009.

- [27] M.J. Frisch, G.W. Trucks, H.B. Schlegel, G.E. Scuseria, M.A. Robb, J.R. Cheeseman Jr., J.A. Montgomery, T. Vreven, K.N. Kudin, J.C. Burant, J.M. Millam, S.S. Iyengar, J. Tomasi, V. Barone, B. Mennucci, M. Cossi, G. Scalmani, N. Rega, G.A. Petersson, H. Nakatsuji, M. Hada, M. Ehara, K. Toyota, R. Fukuda, J. Hasegawa, M. Ishida, T. Nakajima, Y. Honda, O. Kitao, H. Nakai, M. Klene, X. Li, J.E. Knox, H.P. Hratchian, J.B. Cross, V. Bakken, C. Adamo, J. Jaramillo, R. Gomperts, R.E. Stratmann, O. Yazyev, A.J. Austin, R. Cammi, C. Pomelli, J.W. Ochterski, P.Y. Ayala, K. Morokuma, G.A. Voth, P. Salvador, J.J. Dannenberg, V.G. Zakrzewski, S. Dapprich, A.D. Daniels, M. C. Strain, O. Farkas, D.K. Malick, A.D. Rabuck, K. Raghavachari, J.B. Foresman, J. V. Ortiz, Q. Cui, A.G. Baboul, S. Clifford, J. Cioslowski, B.B. Stefanov, G. Liu, A. Liashenko, P. Piskorz, I. Komaromi, R.L. Martin, D.J. Fox, T. Keith, M.A. Al-Laham, C.Y. Peng, A. Nanayakkara, M. Challacombe, P.M.W. Gill, B. Johnson, W. Chen, M.W. Wong, C. Gonzalez, J.A. Pople, Gaussian 03W, Gaussian Inc., Wallingford, CT, 2004.
- [28] A.D. Becke, *J. Chem. Phys.* 98 (1993) 5648-5652.
- [29] C. Lee, W. Yang, R. Parr, *Phys. Rev.* 37 (1988) 785-789.
- [30] K. Fukui, *Angewandte Chemie International Edition in English.* 21 (1982) 801-809.
- [31] R.G. Parr, R.G. Pearson, *J. Am. Chem. Soc.* 105 (1983) 7512-7516.
- [32] R.G. Pearson, *Inorg. Chem.* 27 (1988) 734-740.
- [33] W. Yang, R.G. Parr, *Proc. Natl. Acad. Sci.* 82 (1985) 6723-6726.
- [34] T. Koopmans, *Physica* 1 (1933) 104-113.
- [35] R.G. Parr, L.v. Szentpaly, S. Liu, *J. Am. Chem. Soc.* 121 (1999) 1922-1924.
- [36] I.B. Obot, S. Kaya, C. Kaya, B. Tüzün, *Physica E: Low Dimensional Systems and Nanostructures.* 80 (2016) 82-90.
- [37] A. Popova, M. Christov, T. Deligeorgiev, *Corrosion.* 59 (2003) 756-764.
- [38] G. Bereket, E. Hür, C. Öğretir, *J. Mol. Struct: THEOCHEM.* 578 (2002) 79-88.
- [39] I.B. Obot, N.O. Obi-Egbedi, *Corr. Sci.* 52 (2010) 198-204.
- [40] L. Guo, S. Zhu, S. Zhang, Q. He, W. Li, *Corr. Sci.* 87 (2014) 366-375.
- [41] S. Kirkpatrick, C.D. Gelatt, M.P. Vecchi, *Science* 220 (1983) 671-680.
- [42] R.G. Pearson, *J. Am. Chem. Soc.* 85 (1963) 3533-3539.
- [43] S. Martinez, *Mater. Chem. Phys.* 77 (2003) 97-102.
- [44] M.J.S. Dewar, W. Thiel, *J. Am. Chem. Soc.* 3533.
- [45] I. Lukovits, E. Kalman, F. Zucchi, *Corrosion.* 57 (2001) 3-8.
- [46] B. Gomez, N.V. Likhanova, M.A. Dominguez-Aguilar, R. Martinez-Palou, A. Vela, J.L. Gazquez, *J. Phys. Chem. B.* 110 (2006) 8928-8934.
- [47] V.R. Saliyan, A.V. Adhikari, *Corr. Sci.* 50 (2008) 55-61.
- [48] M El Faydy, N Dahaieh, K Ounine, B Lakhrissi, I Warad, B Tüzün, A Zarrouk, *Arabian Journal for Science and Engineering*, (2021) 1-14
- [49] A.T. Bilgiçli, H.G. Bilgicli, C. Hepokur, B. Tüzün, A. Günsel, M. Zengin, M.N. Yarasir, *Applied Organometallic Chemistry*, (2021) e6242

[50] E Önem, B Tüzün, S Akkoç, Journal of Biomolecular Structure and Dynamics (2021) 1-12

[51] V.S. Sastri, J.R. Perumareddi, Corrosion. 53 (1997) 617-622.

[52] B.J. Smith, L. Radom, J. Phys. Chem. 99 (1995) 6468-6471.

IntechOpen

IntechOpen